SUPERCONDUCTING CYCLOTRON PROJECT AT VECC

Rakesh Kumar Bhandari (for the VECC Staff)
Variable Energy Cyclotron Centre, I/AF Bidhan Nagar, Kolkata-700 064, India

Abstract

Construction of the K-500 superconducting cyclotron at Kolkata is now in final stages. The main magnet was operated satisfactorily for almost one year during 2005-2006. The coil was continuously kept cooled at 4.5K temperature during the entire period. Extensive magnetic field measurements were done for correction of the imperfections, centering of the main coil, calculation of operational settings, calculation of extraction trajectory etc. Subsequently, in April 2006 the coil has been warmed up to facilitate assembly of other systems of the machine. All major systems have been fabricated and the assembly is currently going on. We plan to start the commissioning tests later in the year 2007. In this paper our experience with the operation of the main superconducting magnet and magnetic field measurements will be discussed. Developmental highlights of various systems will be briefly presented.

INTRODUCTION

The main magnet of the superconducting cyclotron is designed to operate at about 800A current in each α as well as β coil producing a maximum of about 6T magnetic field [1]. The main magnet iron structure, weighing about 80 tonnes, along with superconducting coil and cryostat had been installed at the new cyclotron building in later part of 2004. The liquid He plant, cryogenic delivery system, power supplies and the control systems were successfully commissioned. The magnet was cooled down to liquid He temperature and energised first time in the early 2005.

In the subsequent months, the magnet was operated satisfactorily for almost one year. The coil was continuously kept cooled at 4.5 K temperature during the entire period. Extensive magnetic field measurements were done for correction of the manufacturing defects and assembly errors in the iron structure, centering of the main coil, calculation of operational settings, calculation of extraction trajectory etc. After completion of magnetic field measurement activity in April 2006, the coil was warmed up to facilitate assembly of the RF system and other major systems of the machine. All major components of the RF system have been fabricated and the assembly work is currently going on. The installation of ECR ion source has been started. Installation work of injection beam line has also started.

INSTALLATION AND COMMISSIONING OF DIFFERENT SYSTEMS

The superconducting magnet along with cryogenic delivery system (fig. 1) and other related subsystems was installed by early 2005 [1]. The low carbon iron frame and the annular cryostat, housing Nb-Ti superconducting coil, were assembled and aligned concentrically. The coil is suspended inside the cryostat by nine glass epoxy support links - 6 vertical and 3 radial. The tensile forces on the support links are monitored by strain-gauged-studs. The 200W (at 4.5K) helium refrigerator/liquefier had already been installed alongside the cyclotron building. The transfer lines along with valves, manifolds and sensors have been installed connecting the cold box and nitrogen delivery system to the cryostat. The control system based on industrial PLC and HMI software was commissioned. A turbo-molecular pump, backed by scroll pump, maintains ~10^{-6} mbar pressure in the cryostat outer vacuum chamber. Two 1000A, 20V power supplies with 10-ppm stability for the main coil along with dump resistors and control software have been installed. The magnetic field measurement setup that uses optical encoders for accurate position measurement and stepper and smart motor driver for the search coil was also installed and tested thoroughly.

Figure 1: Main magnet with cryogenic delivery system.

Cooling of the Coil and Cryostat

The moisture level in the liquid helium chamber was reduced below 10 ppm, before starting the cool down process, by repetitive evacuation and purging with pure helium gas and heating the coil with 5A current. Then the temperature was brought down by sending cold helium gas from the plant to the cryostat. Initially, the liquid nitrogen flow to the radiation shield was not available. Still the liquid helium plant was capable enough to cool

the coil to 4.5K and to immerse it with liquid helium (fig. 2). Subsequently, the liquid nitrogen flow to the shield was provided. Some leaks were detected on the current lead bellows during cooling down and those were fixed.

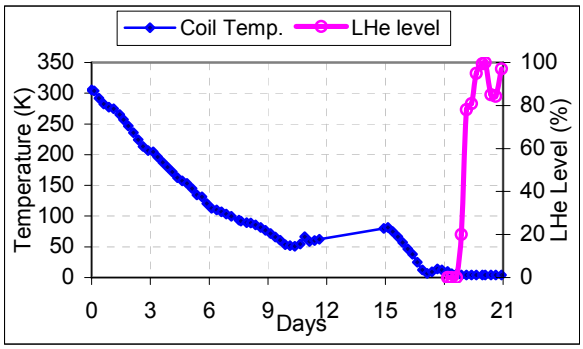

Figure 2: Coil temperature and liquid He level vs. time during the cool down.

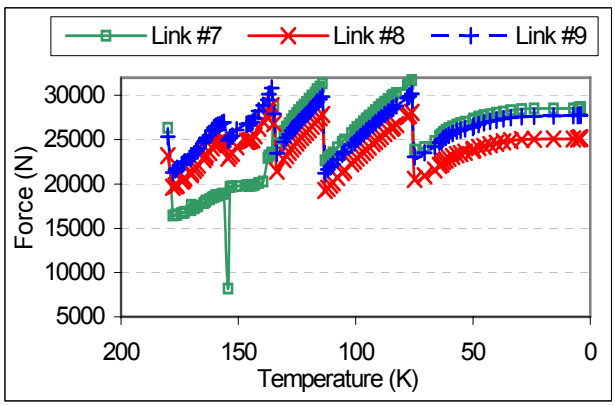

Figure 3: Radial support link forces during cool down.

During the cool down, the radial support link forces were adjusted to keep the forces within safe limits. At 154.4K temperature, the safety nut of the link #7 happened to share the entire load instead of the strain gauge stud due to a human error. This is indicated as a sharp dip in fig. 3. Liquid He boil-off measurement was carried out to find out the cryostat heat load (≈23W).

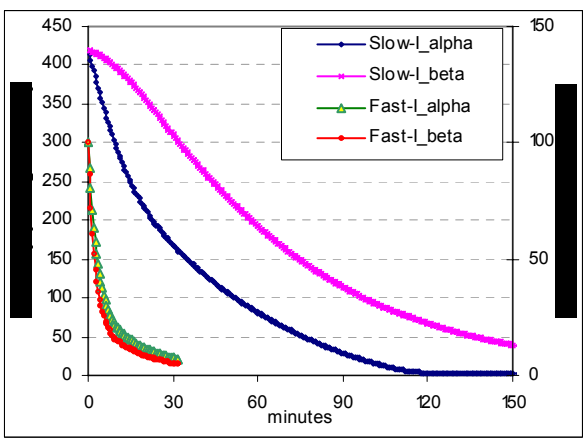

Figure 4: Slow-dump and fast-dump decay curves.

Magnet Excitation

After stabilizing the required liquid helium level in the cryostat for a couple of weeks, the magnet excitation was initiated. All the safety interlock systems were tested by forcing the coil current decay through slow and fast dump resistors (fig. 4). Several iterations were required for coil the centering process and adjustment of plant parameters before reaching 550A current and 4.8T magnetic field at 33 cm radius in the hill region (fig. 5).

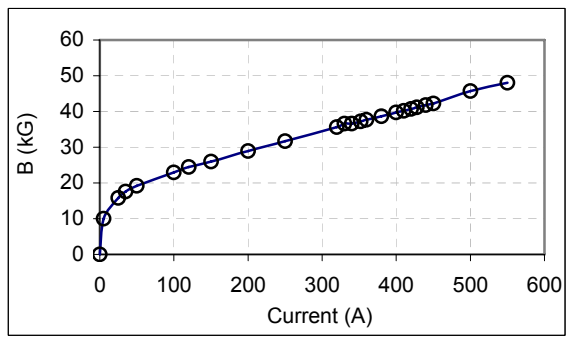

Figure 5: Magnetic field at 33 cm radius in hill region.

Coil Centering

The coil experiences position and current dependent force that was observed as change in the radial support link force. The coil needs to be moved to a position where the coil axis matches with the magnetic axis of symmetry. At this position, the forces on the radial support links decrease monotonically with current due to expansion of the coil in response to the magnetic hoop stresses as shown in fig. 6.

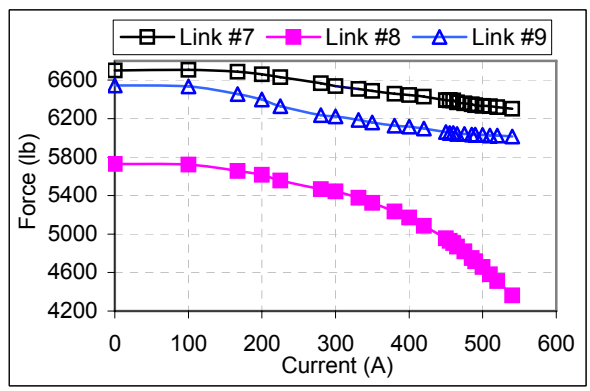

Figure 6: Radial support link forces vs. coil current.

Magnetic Field Measurements

Extensive magnetic field mapping has been done at different main coil excitations. The field has been measured with a search coil and NMR (for calibration) set up, with linear and angular positioning accuracy of 10 μm and 0.5 arc-seconds, respectively. The required field uniformity to lock the NMR signal was found at the centre of the magnet and near the RF holes in the valley region as shown by contour plots with 10 G step in figure 7 a & b.

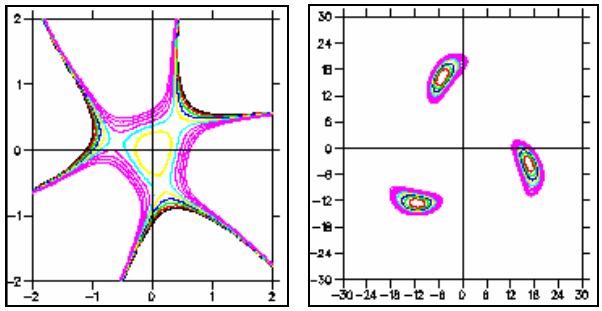

Figure 7: (a) Contour plots of magnetic field at the centre, (b) contour plots near the three RF holes showing the uniform field regions where NMR signal locked.

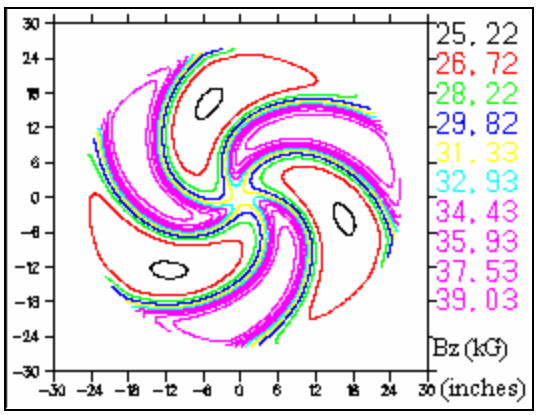

Figure 8: Isogauss contour plot of the measured field.

Three-fold symmetry dominated magnetic field is characteristic feature of the three-sector geometry of our superconducting cyclotron magnet as shown in fig. 8. Deviation from perfect three-fold symmetry arises out of manufacturing and assembly errors, as shown by the contour plot of all error harmonics in fig. 9.

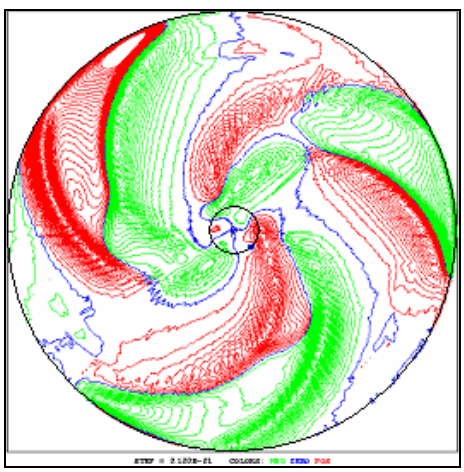

Figure 9: Error harmonics other than 3rd harmonic and those multiple of 3.

Average Field Correction

The radial distribution of the average field (B_{av}) for different current settings (I_α, I_β) is shown in fig 10. Iron shims were added to remove unwanted dips in the average iron field at about 4", 7" and 14" radii (fig. 11). The positions of these shims are shown in fig. 12.

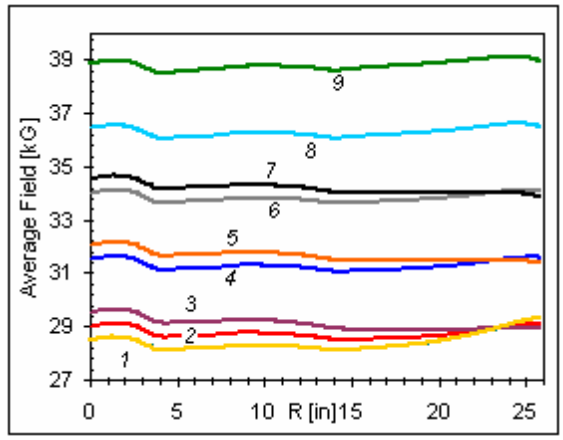

Figure 10: Average field for following main coil excitations (I_{alpha}, I_{beta}). 1: (475, 175), 2: (425, 225), 3: (375, 275), 4: (453, 290), 5: (403, 340), 6: (481, 356), 7: (509, 422), 8: (459, 472), 9: (537, 487).

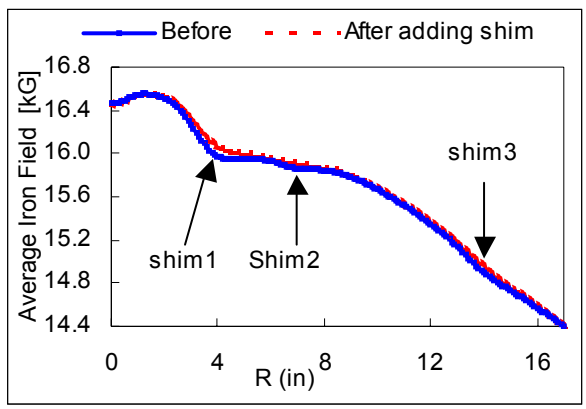

Figure 11: Correction of errors in the average field.

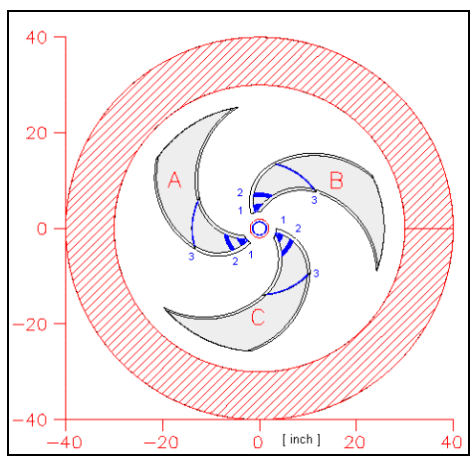

Figure 12: Shim positions for B_{av} correction (dark strips).

First Harmonic Correction

Minimization of 1st harmonic component in the field is one of the most important motives of the field measurement activity. The radial distributions of 1st harmonic component at different stages of corrections are

shown in fig. 13 as Map1, Map2 and Map3. The 1st harmonic amplitude and phase distribution were carefully investigated to determine the size and position of the iron shims. One of the observations was the movement of the pole-tips when magnet was excited. Culprits were faulty bolts. It was detected by the measurements and were replaced with some difficulty. The final positions of the shims are shown in fig. 14. We could limit the 1st harmonic component to within 7 gauss near the extraction radius, which can be adequately handled during the beam extraction process with the help of the trim coil #13.

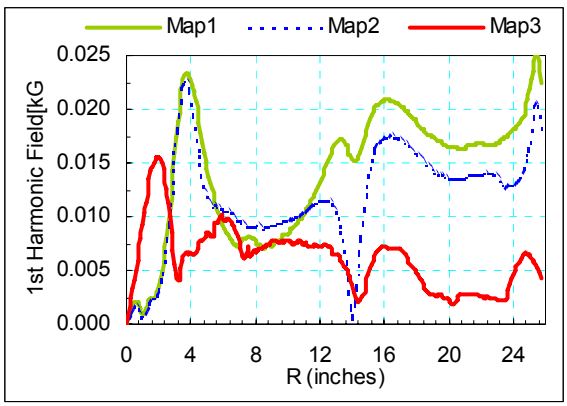

Figure 13: Minimization of 1st harmonic in the main field.

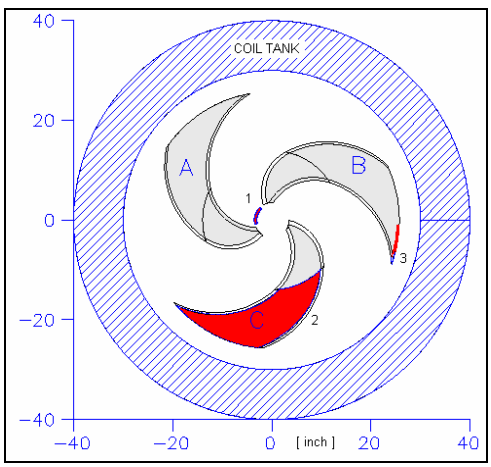

Figure 14: Shim positions for 1st harmonic correction.

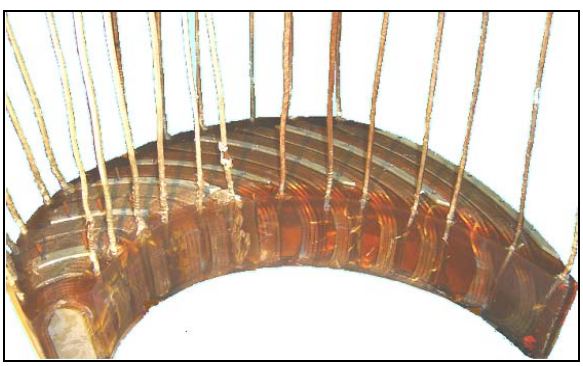

Figure 15: Trim coils placed on the pole tip.

Trim coils

After completion of the magnetic field measurements, the magnet has been disassembled to install the trim coils, RF resonators and other systems. There are 13 epoxy potted trim coils wound on each pole tip as shown in the fig. 15. The trim coil assembly work has been completed.

Installation of RF System

All the three RF amplifiers have been installed in the cyclotron vault and tested. Fig. 16 shows the Q-value of one of the amplifier cavities measured using a vector network analyser.

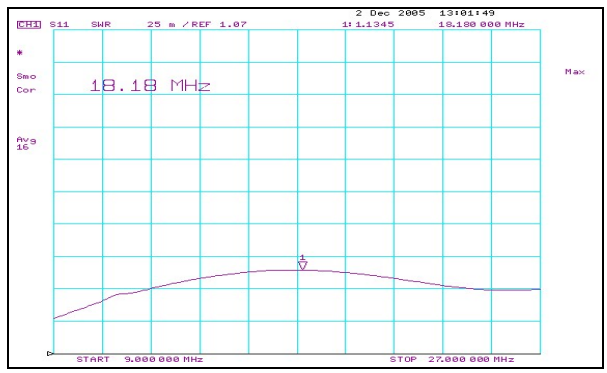

Figure 16: Loaded Q is >100 in the entire frequency range of 9–27 MHz, indicating at least 20dB harmonic rejection.

A significant part of the RF resonator system has been assembled on the bench and final assembly work in the cyclotron is in progress. Figs. 17 to 20 show important parts of the RF amplifier and resonator system. The RF liners are also undergoing vacuum and hydraulic tests. We expect to complete the assembly of the entire RF cavity very soon. The commissioning of the RF system is expected to start by mid 2007.

Figure 17: Assembly of screen bypass capacitor with tetrode tube (left) and upper half of one of the three dees (right).

Other Systems

The cryopanels for cyclotron main vacuum chamber are in the final stages of fabrication. The cryogenic delivery system for the cryopanels is presently being installed in the cyclotron vault.

Figure 18: Sliding short assembly with Be-Cu contact fingers.

Figure 19: One of the six RF resonators being assembled at VECC.

Figure 20: RF liner assemblies ready for installation.

Injection and Extraction Beam Lines

The ECR ion source is being installed in the high bay of the superconducting cyclotron building. Most of the components of the injection beam line are also ready for installation. Fig. 21 shows the injection scheme with two ECR ion sources. Layout of the external beam lines is shown in fig. 22.

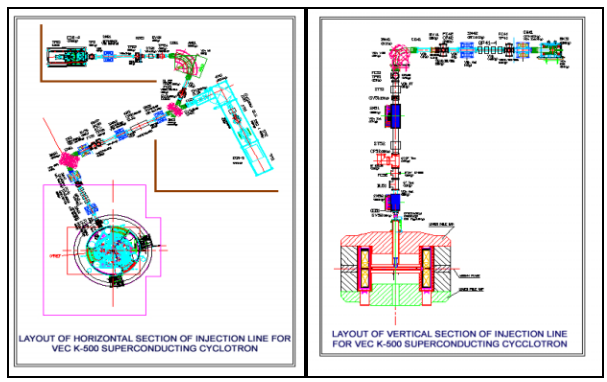

Figure 21: Horizontal and vertical views of the injection beam lines with two ECR sources.

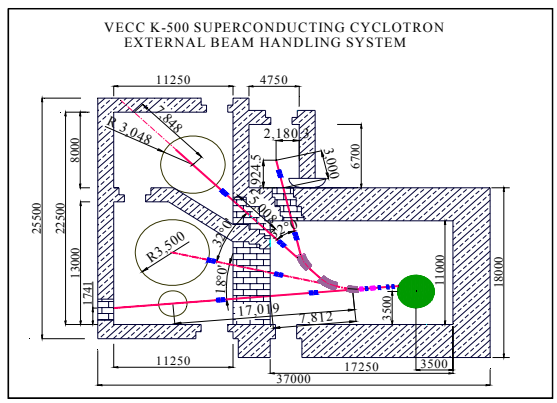

Figure 22: External beam lines layout for the VECC superconducting cyclotron. There are three beam lines for nuclear physics and one for irradiation experiments.

CONCLUSIONS

Most important component of the cyclotron i.e. the superconducting magnet has already been commissioned. Other systems are currently being assembled. Commissioning tests will start before the end of 2007.

ACKNOWLEDGEMENT

Construction of the superconducting cyclotron is a combined effort of several dedicated scientists, engineers and administrative staffs of the Centre. Their contributions are gratefully acknowledged.

REFERENCES

[1] R. K. Bhandari, "Status of the K-500 Superconducting Cyclotron", Proc. of Indian Particle Accelerator Conference (InPAC-2005), Kolkata, March 1-5, 2005, p. 1.